

Gate-induced superconductivity in atomically thin MoS₂ crystals

Davide Costanzo¹, Sanghyun Jo¹, Helmuth Berger² and Alberto F. Morpurgo^{1*}

When thinned down to the atomic scale, many layered van der Waals materials exhibit an interesting evolution of their electronic properties, whose main aspects can be accounted for by changes in the single-particle bandstructure. Phenomena driven by interactions are also observed, but identifying experimentally systematic trends in their thickness dependence is challenging. Here, we explore the evolution of gate-induced superconductivity in exfoliated MoS₂ multilayers ranging from bulk-like to individual monolayers. We observe a clear transition for all thicknesses down to the ultimate atomic limit, providing the first demonstration of gate-induced superconductivity in atomically thin exfoliated crystals. Additionally, we characterize the superconducting state by measuring the critical temperature T_C and magnetic field B_C in a large number of multilayer devices while decreasing their thickness. We find that the superconducting properties exhibit a pronounced reduction in T_C and B_C when going from bilayers to monolayers, for which we discuss possible microscopic mechanisms.

The ability to produce few-atoms-thick two-dimensional materials of excellent quality^{1,2}, such as graphene^{3–5}, semiconducting transition-metal dichalcogenides (TMDs)^{6,7} and phosphorene⁸, is an impressive breakthrough in condensed-matter physics and nanoelectronics. On adding an individual monolayer to such a two-dimensional material, its electronic properties change drastically, demonstrating that multilayers of different thickness truly represent distinct electronic systems^{9–12}. The basic aspects of their thickness-dependent properties are usually captured well by single-particle bandstructure calculations^{13–16}. Depending on the specific system, the experimental conditions and the physical processes investigated, interaction effects can also play an important role. Examples include excitonic effects^{17–19} and gap renormalization in semiconducting TMDs²⁰, or the transport properties of few-layer, suspended graphene very close to charge neutrality^{21–23}. Compared with the properties described by a single-particle picture, exploring the thickness dependence of phenomena in which interactions play a key role is considerably more complex²⁴, and only limited work has been done to date. Here, we report the investigation of one such phenomenon—gate-induced superconductivity—in MoS₂ multilayers with thickness ranging from six monolayers to one monolayer, and reveal a systematic behaviour of the key properties characterizing the superconducting state, such as critical temperature (T_C) and field (B_C).

Early pioneering studies aimed at probing superconductivity in individual layers of superconducting TMDs date back to the 1970s^{25,26}, but only over the last few years the experimental control necessary to unambiguously identify the thickness of atomically thin layers has been developed. For gate-induced superconductivity at the surface of semiconducting TMDs, this has been demonstrated recently using MoS₂ field-effect transistors²⁷ (FETs) with liquid gates^{28–30}, in breakthrough work performed on thick exfoliated layers behaving in all regards as bulk. This work has led to the observation of T_C values up to 12 K following the accumulation of electron surface densities close to $n \approx 1 \times 10^{14} \text{ cm}^{-2}$. The relatively high critical temperature and the possibility to obtain chemically stable monolayers by simple exfoliation techniques make MoS₂ an ideal choice to investigate the evolution of

gate-induced superconductivity on reducing its thickness down to the atomic scale.

Gate-induced superconductivity in thick multilayers

Figure 1a presents an optical microscope image of a typical device implemented on six-layer (6 L) MoS₂ that is ready to be covered with ionic liquid (see scheme in Fig. 1b). On sweeping the gate voltage V_G for positive values, electrons are accumulated, resulting in an increase in surface conductivity (Fig. 1c). At room temperature, measurements using different contact pairs as voltage probes give the same conductivity values (compare the three curves in Fig. 1c), which is indicative of good device uniformity. This is the typical behaviour of FETs based on MoS₂ multilayers of all thicknesses. To investigate the occurrence of superconductivity, we biased the ionic-liquid FET at $T \approx 220 \text{ K}$ by applying a gate voltage $V_G \approx 2\text{--}5 \text{ V}$ (the precise values depended on the specific device) before cooling it down slowly to $T = 1.5 \text{ K}$. Figure 1d compares the temperature dependence of the resistance below $T = 15 \text{ K}$ measured on a 6 L devices with different contact pairs and in multiple cooldowns, at comparable carrier densities ($1 \times 10^{14} \text{ cm}^{-2}$ to $3 \times 10^{14} \text{ cm}^{-2}$). The expected superconducting transition is present in all curves and manifests itself as a sharp drop in the resistance (albeit not to the $R = 0$ state), which is shifted to lower temperature (and eventually entirely suppressed) by the application of a perpendicular magnetic field (Fig. 1e).

The observed variations in the $R(T)$ curves and T_C measured with different pairs of contacts are a manifestation of the carrier density inhomogeneity that invariably appears at low temperatures in these devices, very probably caused by the frozen ionic liquid locally detaching from the surface of the MoS₂ (as we have recently discussed in more detail for WS₂ ionic-liquid-gated FETs³¹). Despite this inhomogeneity, measurements on 6 L MoS₂ exhibited a clear superconducting transition in each of the cooldowns we performed, whenever n was $\sim 1 \times 10^{14} \text{ cm}^{-2}$ or slightly larger (typically between $1 \times 10^{14} \text{ cm}^{-2}$ and $3 \times 10^{14} \text{ cm}^{-2}$). The measured values of T_C —ranging from 8 to 12 K—are in good agreement with the values of T_C reported in ref. 27 for the same interval of density. The same is

¹DQMP and GAP, Université de Genève, 24 quai Ernest Ansermet, Geneva CH-1211, Switzerland. ²Institut de Physique de la Matière Complexe, Ecole Polytechnique Fédérale de Lausanne, Lausanne CH-1015, Switzerland. *e-mail: alberto.morpurgo@unige.ch

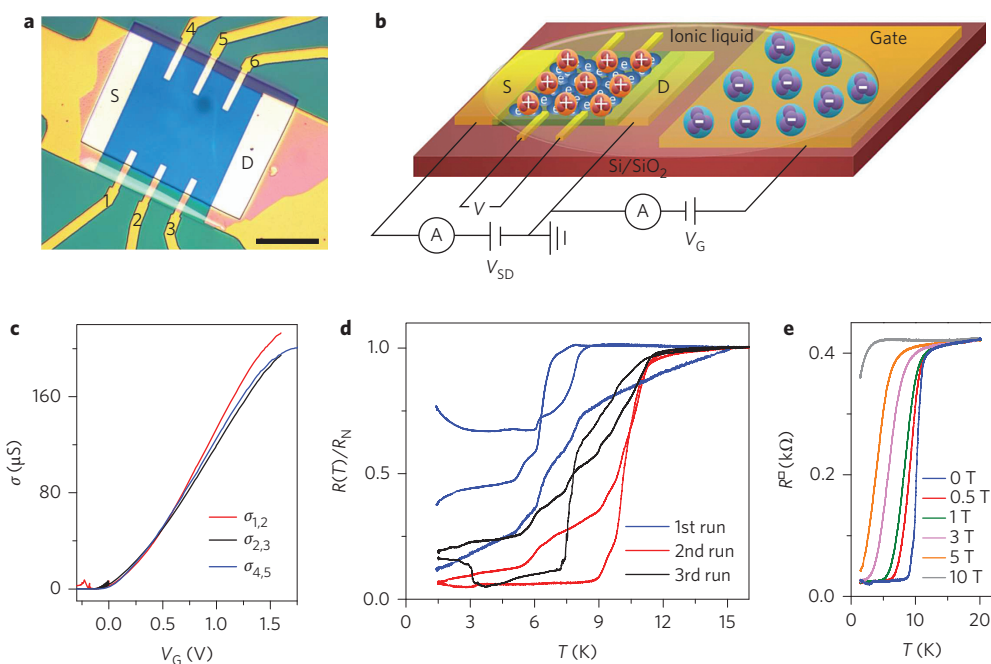


Figure 1 | Device characteristics and superconductivity in an ionic-liquid-gated six-layer MoS₂ transistor. **a**, Optical microscope image of a 6 L MoS₂ FET before deposition of the ionic liquid. Scale bar, 15 μm. In the experiments, current is sent from the source (S) to the drain (D) electrode, and different voltage probes (labelled 1 to 6) are used to measure the voltage. **b**, Schematic illustration of ionic-liquid-gated FETs, under electron accumulation. **c**, Gate voltage (V_G) dependence of room-temperature conductivity measured in different four-probe configurations ($\sigma_{A,B}$ indicates the conductivity obtained from the voltage drop measured with probes A and B). The data show that, above the freezing temperature of the ionic liquid, the device exhibits homogeneous behaviour. **d**, Temperature dependence of the (normalized) four-probe resistance at high electron density ($n \approx 1 \times 10^{14} \text{ cm}^{-2}$) with clear manifestations of the superconducting transition. Different colours correspond to data taken in different cooldowns. The broad transitions and the T_C variations observed when measuring with different contact pairs are due to inhomogeneity arising from the local detachment of the frozen ionic liquid. **e**, A progressive suppression of the transition is observed on increasing the perpendicular magnetic field, substantiating the occurrence of superconductivity (the critical field in this device is $B_C \approx 7 \text{ T}$). R^{\square} , square resistance.

true for the measured perpendicular critical field B_C (we observed values up to 10 T at $T = 1.5 \text{ K}$). We conclude that 6 L MoS₂ multilayers behave in all regards as bulk crystals in terms of gate-induced superconductivity.

Superconductivity persists at the single-layer limit

Having established the occurrence of robust gate-induced superconductivity in 6 L MoS₂, we now discuss the behaviour of thinner multilayers. Figure 2a shows the low-temperature $R(T)$ curves measured at different magnetic fields B on a monolayer device, exhibiting a clear superconducting transition to a $R = 0 \Omega$ state. The response of the same device to a perpendicular magnetic field (at $T = 1.5 \text{ K}$) is shown in Fig. 2b. These observations demonstrate that gate-induced superconductivity in MoS₂ persists all the way down to the ultimate atomic scale. Compared with 6 L MoS₂, the observed critical temperature is significantly lower (the transition onset is just above 2 K) and the superconducting state disappears at much smaller B values ($B_C \approx 0.05\text{--}0.1 \text{ T}$, compared with 5–10 T for the 6 L device, see Fig. 1e; the critical field B_C is defined as the magnetic field for which the measured resistance equals half of that in the normal state just above T_C). Moreover, whereas in 6 L MoS₂ gate-induced superconductivity was observed in every cooldown and for all working contact pairs, observing the superconducting state in monolayers is more difficult. In many cases, monolayers exhibited metallic behaviour (Fig. 2e) without a superconducting transition, probably because in these devices T_C is lower than 1.5 K, the lowest temperature accessible in our experiments. Interestingly, in the absence of superconductivity a clear weak-antilocalization signal due to phase-coherent single-electron transport is usually observed on application of a magnetic field, consistent with the strong spin-orbit interaction present in

MoS₂ (ref. 32 and Fig. 2f; a detailed analysis of this phenomenon will be discussed elsewhere).

Evolution of superconductivity with thickness

For bilayers and thicker multilayers, the behaviour of the superconducting transition more closely resembles the one found in bulk-like flakes than the one in monolayers. For instance, in bilayers and thicker layers we have found superconductivity in every device we have cooled down, as long as n is $\sim 1 \times 10^{14} \text{ cm}^{-2}$ or larger. We illustrate this finding with representative data measured on bilayer MoS₂ in Fig. 3. The transition is rather sharp, with an onset close to $T_C = 7 \text{ K}$. It is suppressed by applying a perpendicular magnetic field on the scale of a few tesla (Fig. 3a,b), which is much larger than the critical field found for monolayers. A very pronounced supercurrent is seen, which is progressively suppressed by increasing T or the applied perpendicular magnetic field (see Fig. 3c and its inset). An analogous behaviour is observed for 3 and 4 L MoS₂. This is illustrated in Fig. 4a,b, which directly compares representative $R(T)$ and $R(B)$ curves measured in multilayers of different thickness from 1 to 6 L.

On the basis of these experimental observations we draw two main conclusions. First, gate-induced superconductivity in MoS₂ persists down to the level of individual monolayers, as unambiguously demonstrated by the observation of a zero resistance state (Fig. 2a,b). Second, the gate-induced superconducting state in monolayers is weaker than in thicker multilayers. Specifically, the maximum T_C in monolayers is suppressed compared with all thicker multilayers, and a ‘jump’ from $\sim 6\text{--}7 \text{ K}$ to 2 K is seen (Fig. 4c) from bilayer to monolayer MoS₂. Also, when looking at the critical magnetic field, it is apparent that the values in monolayers are much smaller (by more than one order of magnitude)

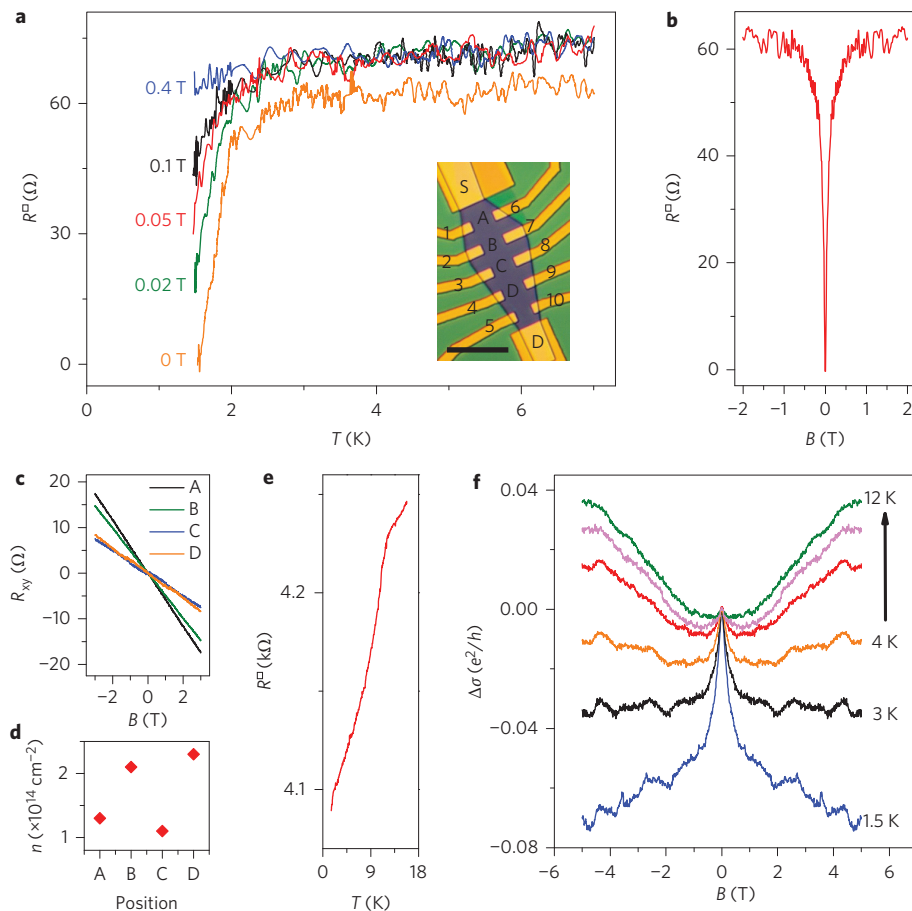


Figure 2 | Gate-induced superconductivity in monolayer MoS₂. **a**, Temperature dependence of four-probe square resistance (R^{\square}) at high electron density ($n \approx 1 \times 10^{14} \text{ cm}^{-2}$) in a monolayer device (inset; scale bar, 15 μm), for different values of perpendicular magnetic field. The sharp drop to zero of the resistance below $T \approx 2 \text{ K}$ at $B = 0 \text{ T}$ demonstrates the occurrence of superconductivity. Despite the accumulation of a high electron density ($n \approx 1 \times 10^{14} \text{ cm}^{-2}$), superconductivity is observed only with one pair of contacts (7–8), in contrast to the 6 L device, in which a superconducting transition is observed irrespective of the contacts used. The superconducting transition is suppressed in a relatively small magnetic field, consistent with the magnetoresistance data shown in **b** (critical field $B_C \approx 0.1 \text{ T}$). **c,d**, Hall effect measurements (**c**) and corresponding carrier density (**d**) measured with different pairs of contacts at positions A, B, C and D (defined in the inset of **a**), showing fluctuations in carrier density. **e,f**, When superconductivity is not observed, a metallic behaviour of the resistance on lowering the temperature is visible (**e**), and the magnetoconductivity exhibits a clear weak antilocalization behaviour (**f**).

than those extracted from all thicker multilayers (Fig. 4d). As for the validity of this last conclusion, we note that a large number of devices were measured to ensure that what we claim is not simply due to insufficient statistics in combination with the effects of charge inhomogeneity. Indeed, in five out of five different devices realized on bilayers or thicker multilayers, superconductivity was observed in each of multiple cooldowns (to a total of 10), with T_C larger than 6 K and B_C exceeding 1 T in all cases. In monolayers, in contrast, a fully developed superconducting state with zero resistance ($T_C = 2 \text{ K}$ and $B_C \approx 0.1 \text{ T}$) was observed in one of six devices that were successfully cooled down, and a clear indication of a superconducting transition (a pronounced dip in resistance observed at perpendicular magnetic field values below 0.1 T) in a second one.

Even though the inhomogeneity in carrier density present in our devices prevents us from fully mapping the critical temperature T_C of multilayers as a function of n , our results are in line with the findings reported in ref. 27. Specifically, we find that—irrespective of the layer thickness—gate superconductivity occurs when the accumulated carrier density is in the range $\sim 1 \times 10^{14} \text{ cm}^{-2}$ to $3 \times 10^{14} \text{ cm}^{-2}$, and it is never observed when n is smaller than $5 \times 10^{13} \text{ cm}^{-2}$ to $6 \times 10^{13} \text{ cm}^{-2}$. These values correspond to what is expected from the $T_C(n)$ curve reported in ref. 27 for thick MoS₂ crystals,

which shows that gate-induced superconductivity appears for $n > 6 \times 10^{13} \text{ cm}^{-2}$, and that it is strongest from n just above $1 \times 10^{14} \text{ cm}^{-2}$. At a quantitative level, in thick MoS₂ crystals for n between $8 \times 10^{13} \text{ cm}^{-2}$ and $3 \times 10^{14} \text{ cm}^{-2}$ T_C was found to be 7 K or larger, which is almost exactly what we find in our devices whenever a bilayer or thicker MoS₂ multilayer is used.

Such a quantitative comparison of T_C values underlines once more that the behaviour of gate-induced superconductivity in monolayers—with a measured maximum T_C of only 2 K—deviates from that observed in thicker multilayers and bulk crystals. One may wonder whether the deviation arises because when considering monolayers a proper comparison should be made at the same charge density per layer, rather than at a same total charge density n . This makes a difference because (at the same value of n) in monolayers the density per layer is approximately twice as large as in thicker multilayers, because in the latter the charge penetrates over the electrostatic screening length, which corresponds approximately to the thickness of two layers^{33,34}. Even considering the density per layer, however, does not solve the discrepancy. Assuming that the phase diagram of ref. 27 is valid in all cases (that is, also for monolayers), one would then expect that the maximum T_C in monolayers should occur at $n = 5 \times 10^{13} \text{ cm}^{-2}$ to $6 \times 10^{13} \text{ cm}^{-2}$, and that for a total accumulated carrier density of

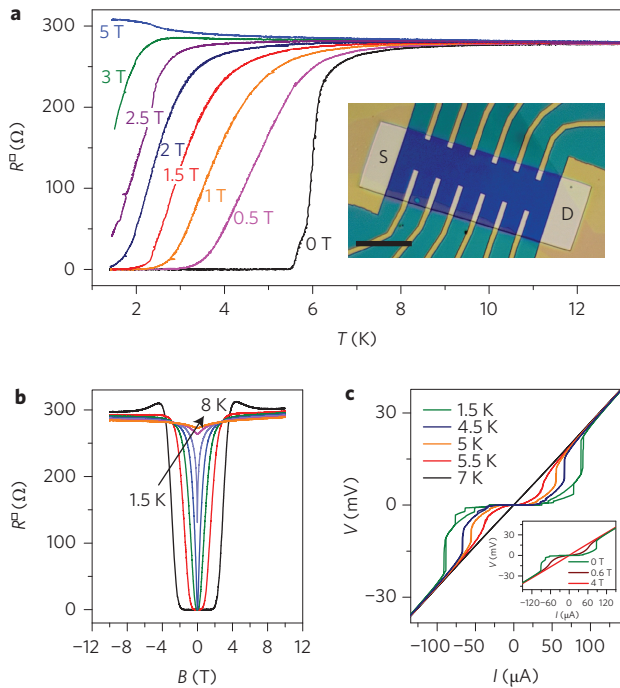


Figure 3 | Superconductivity in bilayer MoS₂. **a**, Temperature dependence of the four-probe square resistance measured at an applied gate voltage of $V_G = 2.2$ V, for different values of perpendicular magnetic field B . At $B = 0$ T, the superconducting transition occurs at $T_C \approx 7$ K, much higher than in the single-layer case, and at $T = 1.5$ K, the zero resistance state remains visible up to $B \approx 2$ T. Inset: optical image of the device. Scale bar, 15 μm . **b**, Magnetoresistance data as a function of temperature. Again, the critical field is much higher than in monolayers. **c**, I - V characteristic showing a pronounced supercurrent at $T = 1.5$ K, which is gradually suppressed on increasing the temperature (or the magnetic field, as shown in the inset).

$n = 1 \times 10^{14} \text{ cm}^{-2}$ to $2 \times 10^{14} \text{ cm}^{-2}$ (the value at which we find the maximum T_C in monolayers) T_C should not be lower than 6 K. Both these expectations are at odds with our experimental observation, because the maximum T_C observed in monolayers occurs at $n = 1 \times 10^{14} \text{ cm}^{-2}$ to $2 \times 10^{14} \text{ cm}^{-2}$ (and not at $n = 5 \times 10^{13} \text{ cm}^{-2}$ to $6 \times 10^{13} \text{ cm}^{-2}$) and is only 2 K (and not 6 K).

Why is superconductivity weaker in monolayers?

The finding that superconductivity is suppressed on reducing the thickness of the material to the level of an individual monolayer may be expected. When the system becomes more two-dimensional, the (thermal and quantum) fluctuations responsible for the suppression of long-range superconducting order become more important^{35,36}. However, a complete understanding requires the identification of specific microscopic mechanisms, and we have identified several different candidates that can play an important major role. The first is associated with the physical thickness of the gate-induced accumulation layer at the surface of MoS₂. This thickness is determined by electrostatic screening, which is estimated to be ~ 1 nm (refs 33,34), as mentioned above. A crossover can therefore be expected when multilayers thinner than the charge accumulation length are used. Because the bilayer thickness is ~ 1.5 nm (ref. 37), such a crossover indeed occurs when going from bilayer to monolayer.

Another mechanism that needs to be considered is the role of the Coulomb interaction between electrons. Superconductivity in MoS₂ is believed to originate from an attractive (phonon-mediated) interaction, the strength of which is reduced by the Coulomb repulsion that is unavoidably present³⁸. On decreasing the thickness of the MoS₂ layer,

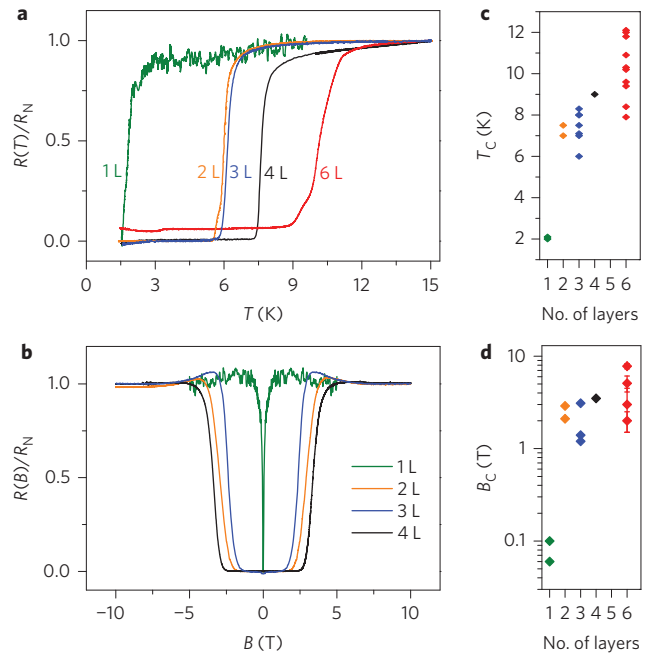


Figure 4 | Evolution of superconductivity in MoS₂ on decreasing the thickness to the atomic scale. **a, b**, Comparison of superconducting transitions in devices of different thickness, from 1 to 6 L, as a function of temperature (**a**) and magnetic field (**b**, at $T = 1.5$ K). **c**, Summary of the critical temperature values measured in MoS₂ devices of different thickness (from 1 to 6 L) at an electron density of $n \approx 1 \times 10^{14} \text{ cm}^{-2}$ or higher. Despite the device-to-device fluctuations, a ‘jump’ in T_C from ~ 7 to 2 K is clearly seen when passing from bilayers to a monolayer (in **c** and **d**, the colour of each symbol indicates the multilayer thickness, according to the same colour code used in **a**). **d**, The behaviour of the critical field (plotted on a log scale) as a function of thickness parallels that of T_C . A one order of magnitude reduction is observed on passing from a bilayer to a monolayer.

electrostatic screening becomes poorer and Coulomb repulsion gains in intensity. Indeed, the relative dielectric constant of thick MoS₂ crystals is $\epsilon \approx 12$ but is $\epsilon \approx 4$ for monolayers^{39,40}, so Coulomb repulsion can be expected to be significantly stronger in monolayers than in thick bulk-like crystals. This leads to a weaker strength of the effective attractive interaction and to a reduced superconducting critical temperature T_C . The effect can be expected to be large, because within the conventional theory of superconductivity T_C depends exponentially on the effective strength of the attractive interaction³⁸.

One more mechanism that appears relevant is related to the specific quantum mechanical states that are occupied by the electrostatically accumulated electrons. There is consensus, based on *ab initio* calculations, that electrons added to the conduction band of MoS₂ monolayers initially fill states close to the K (and K') point^{41–43}, and that for thick multilayers electron accumulation first occurs at the Q point^{12,44,45}, that is, in a different part of the Brillouin zone. At what thickness the transition from K - to Q -point electron accumulation occurs appears to depend on the approximations made in the calculations, but existing results strongly suggest that it takes place when passing from monolayer to bilayer^{12,44–46} (the possibility that it occurs at larger thicknesses is not excluded^{16,47,48}; properly taking into account the large perpendicular electric field unavoidably present at the surface in a transistor configuration is also important⁴⁸). The transition would certainly affect the superconducting state, because the strength of the electron–phonon interaction and the density of states (which determine T_C ⁴⁹) around the K and Q points are different, thus providing a realistic scenario to explain the ‘weaker’ superconductivity observed in MoS₂ monolayers.

It seems clear from all these arguments that the occurrence of superconductivity in thick multilayers does not *a priori* imply that monolayers should also be superconducting. This conclusion reiterates the notion that MoS₂ multilayers of different thickness are in all regards distinct electronic systems, underscoring the relevance of investigating experimentally the thickness dependence of the superconducting transition. In particular, it is not *a priori* correct to analyse the transport properties of charge carriers accumulated at the surface of thick MoS₂ crystals in terms of models appropriate for monolayers (as is sometimes proposed^{50–52}) simply because at high electronic surface densities a large fraction of the carriers are accumulated in the top monolayer. Indeed, our experiments—in conjunction with previous experimental observations²⁷—show that the properties of gate-induced superconductivity in monolayers and at the surface of thicker crystals are distinctly different.

Outlook

Irrespective of these considerations and the specific mechanism responsible for the weakening of the superconducting state in MoS₂ monolayers, the gate-control of superconductivity in atomically thin layers demonstrated here is particularly interesting in the context of so-called van der Waals heterostructures⁵³. In contrast to other interesting systems in which superconductivity has been found to occur in vacuum-deposited, epitaxial films of atomic thickness (such as FeSe^{54,55} and Pb^{56,57}), MoS₂ is fully chemically stable in air, which makes it easy to use for the realization of artificial structures. As demonstrated in different recent experiments, the electronic properties of these structures can be tuned by suitably choosing the sequence of layers that are stacked together⁵³. Including MoS₂ mono- or bilayers in combination with ionic liquid gating adds superconductivity to the phenomena that can be investigated, controlled or used to engineer the electronic properties of van der Waals heterostructures.

Methods

Methods and any associated references are available in the [online version of the paper](#).

Received 11 May 2015; accepted 30 November 2015; published online 11 January 2016

References

- Xu, M., Liang, T., Shi, M. & Chen, H. Graphene-like two-dimensional materials. *Chem. Rev.* **113**, 3766–3798 (2013).
- Butler, S. Z. *et al.* Progress, challenges, and opportunities in two-dimensional materials beyond graphene. *ACS Nano* **7**, 2898–2926 (2013).
- Novoselov, K. S. *et al.* Electric field effect in atomically thin carbon films. *Science* **306**, 666–669 (2004).
- Novoselov, K. S. *et al.* Two-dimensional gas of massless Dirac fermions in graphene. *Nature* **438**, 197–200 (2005).
- Zhang, Y., Tan, Y.-W., Stormer, H. L. & Kim, P. Experimental observation of the quantum Hall effect and Berry's phase in graphene. *Nature* **438**, 201–204 (2005).
- Wang, Q. H., Kalantar-Zadeh, K., Kis, A., Coleman, J. N. & Strano, M. S. Electronics and optoelectronics of two-dimensional transition metal dichalcogenides. *Nature Nanotech.* **7**, 699–712 (2012).
- Chhowalla, M. *et al.* The chemistry of two-dimensional layered transition metal dichalcogenide nanosheets. *Nature Chem.* **5**, 263–275 (2013).
- Li, L. *et al.* Black phosphorus field-effect transistors. *Nature Nanotech.* **9**, 372–377 (2014).
- Castro Neto, A. H., Guinea, F., Peres, N. M. R., Novoselov, K. S. & Geim, A. K. The electronic properties of graphene. *Rev. Mod. Phys.* **81**, 109–162 (2009).
- Koshino, M. & McCann, E. Parity and valley degeneracy in multilayer graphene. *Phys. Rev. B* **81**, 115315 (2010).
- Mak, K. F., Lee, C., Hone, J., Shan, J. & Heinz, T. F. Atomically thin MoS₂: a new direct-gap semiconductor. *Phys. Rev. Lett.* **105**, 136805 (2010).
- Splendiani, A. *et al.* Emerging photoluminescence in monolayer MoS₂. *Nano Lett.* **10**, 1271–1275 (2010).
- Partoens, B. & Peeters, F. M. Normal and Dirac fermions in graphene multilayers: tight-binding description of the electronic structure. *Phys. Rev. B* **75**, 193402 (2007).
- Nilsson, J., Castro Neto, A. H., Guinea, F. & Peres, N. M. R. Electronic properties of bilayer and multilayer graphene. *Phys. Rev. B* **78**, 045405 (2008).
- Cappelluti, E., Roldán, R., Silva-Guillén, J. A., Ordejón, P. & Guinea, F. Tight-binding model and direct-gap/indirect-gap transition in single-layer and multilayer MoS₂. *Phys. Rev. B* **88**, 075409 (2013).
- Cheiwchanchamnangij, T. & Lambrecht, W. R. L. Quasiparticle band structure calculation of monolayer, bilayer, and bulk MoS₂. *Phys. Rev. B* **85**, 205302 (2012).
- Mak, K. F. *et al.* Tightly bound trions in monolayer MoS₂. *Nature Mater.* **12**, 207–211 (2013).
- Chernikov, A. *et al.* Exciton binding energy and nonhydrogenic Rydberg series in monolayer WS₂. *Phys. Rev. Lett.* **113**, 076802 (2014).
- Ye, Z. *et al.* Probing excitonic dark states in single-layer tungsten disulphide. *Nature* **513**, 214–218 (2014).
- Ugeda, M. M. *et al.* Giant bandgap renormalization and excitonic effects in a monolayer transition metal dichalcogenide semiconductor. *Nature Mater.* **13**, 1091–1095 (2014).
- Elias, D. C. *et al.* Dirac cones reshaped by interaction effects in suspended graphene. *Nature Phys.* **7**, 701–704 (2011).
- Velasco, J. *et al.* Transport spectroscopy of symmetry-broken insulating states in bilayer graphene. *Nature Nanotech.* **7**, 156–160 (2012).
- Grushina, A. L. *et al.* Insulating state in tetralayers reveals an even–odd interaction effect in multilayer graphene. *Nature Commun.* **6**, 6419 (2015).
- Yoshida, M. *et al.* Controlling charge-density-wave states in nano-thick crystals of 1T-TaS₂. *Sci. Rep.* **4**, 7302 (2014).
- Frindt, R. F. Superconductivity in ultrathin NbSe₂ layers. *Phys. Rev. Lett.* **28**, 299–301 (1972).
- Gamble, F. R., Osiecki, J. H., Cais, M. & Pisharody, R. Intercalation complexes of Lewis bases and layered sulfides: a large class of new superconductors. *Science* **174**, 493–497 (1971).
- Ye, J. T. *et al.* Superconducting dome in a gate-tuned band insulator. *Science* **338**, 1193–1196 (2012).
- Panzer, M. J., Newman, C. R. & Frisbie, C. D. Low-voltage operation of a pentacene field-effect transistor with a polymer electrolyte gate dielectric. *Appl. Phys. Lett.* **86**, 103503 (2005).
- Shimotani, H., Asanuma, H., Takeya, J. & Iwasa, Y. Electrolyte-gated charge accumulation in organic single crystals. *Appl. Phys. Lett.* **89**, 203501 (2006).
- Misra, R., McCarthy, M. & Hebard, A. F. Electric field gating with ionic liquids. *Appl. Phys. Lett.* **90**, 052905 (2007).
- Jo, S., Costanzo, D., Berger, H. & Morpurgo, A. F. Electrostatically induced superconductivity at the surface of WS₂. *Nano Lett.* **15**, 1197–1202 (2015).
- Ochoa, H., Finocchiaro, F., Guinea, F. & Fal'ko, V. I. Spin–valley relaxation and quantum transport regimes in two-dimensional transition-metal dichalcogenides. *Phys. Rev. B* **90**, 235429 (2014).
- Horowitz, G., Hajlaoui, M. E. & Hajlaoui, R. Temperature and gate voltage dependence of hole mobility in polycrystalline oligothiophene thin film transistors. *J. Appl. Phys.* **87**, 4456–4463 (2000).
- Saito, Y. *et al.* Superconductivity protected by spin-valley locking in ion-gated MoS₂. *Nature Phys.* <http://dx.doi.org/10.1038/nphys3580> (2015).
- Berezinskii, V. L. Destruction of long-range order in one-dimensional and two-dimensional systems having a continuous symmetry group I. classical systems. *Sov. J. Exp. Theor. Phys.* **32**, 493–500 (1971).
- Kosterlitz, J. M. & Thouless, D. J. Ordering, metastability and phase transitions in two-dimensional systems. *J. Phys. C Solid State Phys.* **6**, 1181–1203 (1973).
- Radisavljevic, B., Radenovic, A., Brivio, J., Giacometti, V. & Kis, A. Single-layer MoS₂ transistors. *Nature Nanotech.* **6**, 147–150 (2011).
- Scalapino, D. J. in *Superconductivity* Vol. 1 (ed. Parks, R. D.) Ch. 10, 449–560 (Marcel Dekker, 1969).
- Santos, E. J. G. & Kaxiras, E. Electrically driven tuning of the dielectric constant in MoS₂ layers. *ACS Nano* **7**, 10741–10746 (2013).
- Chen, X. *et al.* Probing the electron states and metal–insulator transition mechanisms in molybdenum disulphide vertical heterostructures. *Nature Commun.* **6**, 6088 (2015).
- Li, T. & Galli, G. Electronic properties of MoS₂ nanoparticles. *J. Phys. Chem. C* **111**, 16192–16196 (2007).
- Lebègue, S. & Eriksson, O. Electronic structure of two-dimensional crystals from *ab-initio* theory. *Phys. Rev. B* **79**, 115409 (2009).
- Ge, Y. & Liu, A. Y. Phonon-mediated superconductivity in electron-doped single-layer MoS₂: a first-principles prediction. *Phys. Rev. B* **87**, 241408 (2013).
- Kuc, A., Zibouche, N. & Heine, T. Influence of quantum confinement on the electronic structure of the transition metal sulfide TS₂. *Phys. Rev. B* **83**, 245213 (2011).
- Ellis, J. K., Lucero, M. J. & Scuseria, G. E. The indirect to direct band gap transition in multilayered MoS₂ as predicted by screened hybrid density functional theory. *Appl. Phys. Lett.* **99**, 261908 (2011).
- Jiang, T. *et al.* Valley and band structure engineering of folded MoS₂ bilayers. *Nature Nanotech.* **9**, 825–829 (2014).
- Zahid, F., Liu, L., Zhu, Y., Wang, J. & Guo, H. A generic tight-binding model for monolayer, bilayer and bulk MoS₂. *AIP Adv.* **3**, 052111 (2013).

48. Brumme, T., Calandra, M. & Mauri, F. First-principles theory of field-effect doping in transition-metal dichalcogenides: structural properties, electronic structure, Hall coefficient, and electrical conductivity. *Phys. Rev. B* **91**, 155436 (2015).
49. Schrieffer, J. R. *Theory of Superconductivity* (Advanced Books, 1999).
50. Morpurgo, A. F. Spintronics: gate control of spin-valley coupling. *Nature Phys.* **9**, 532–533 (2013).
51. Yuan, H. *et al.* Zeeman-type spin splitting controlled by an electric field. *Nature Phys.* **9**, 563–569 (2013).
52. Lu, J. M. *et al.* Evidence for two-dimensional Ising superconductivity in gated MoS₂. *Science*. **350**, 1353–1357 (2015).
53. Geim, A. K. & Grigorieva, I. V. Van der Waals heterostructures. *Nature* **499**, 419–425 (2013).
54. Qing-Yan, W. *et al.* Interface-induced high-temperature superconductivity in single unit-cell FeSe films on SrTiO₃. *Chin. Phys. Lett.* **29**, 37402 (2012).
55. Ge, J.-F. *et al.* Superconductivity above 100 K in single-layer FeSe films on doped SrTiO₃. *Nature Mater.* **14**, 285–289 (2015).
56. Zhang, T. *et al.* Superconductivity in one-atomic-layer metal films grown on Si(111). *Nature Phys.* **6**, 104–108 (2010).
57. Sekihara, T., Masutomi, R. & Okamoto, T. Two-dimensional superconducting state of monolayer Pb films grown on GaAs(110) in a strong parallel magnetic field. *Phys. Rev. Lett.* **111**, 057005 (2013).

Acknowledgements

The authors thank A. Ferreira for technical help and T. Giamarchi, F. Mauri and M. Calandra for useful discussions. The authors acknowledge the Swiss National Science Foundation (SNF) and the EU Graphene Flagship Project for financial support.

Author contributions

D.C. fabricated the majority of the devices and performed most of the measurements, with assistance and supervision from S.J. D.C. and S.J. analysed the data. H.B. provided the MoS₂ crystals. A.F.M. proposed the experiment and supervised the research. All authors discussed the results and contributed to their interpretation. D.C., S.J. and A.F.M. wrote the manuscript.

Additional information

Supplementary information is available in the [online version](#) of the paper. Reprints and permissions information is available online at www.nature.com/reprints. Correspondence and requests for materials should be addressed to A.F.M.

Competing financial interests

The authors declare no competing financial interests.

Methods

Device fabrication. Flakes of MoS₂ multilayers of different thickness were mechanically exfoliated from a bulk crystal using adhesive tape, then transferred onto a Si/SiO₂ substrate. The thickness of the flakes was identified by measuring their optical contrast, in conjunction with atomic force microscopy and photoluminescence measurements. Au electrodes (50 nm) were patterned by conventional nanofabrication techniques (electron-beam lithography, metal evaporation and liftoff) and annealed at 200 °C for 2 h in a flow of an Ar/H₂ (100/10 s.c.c.m.) mixture to reduce the contact resistance. Together with the electrodes, a large Au pad acting as a gate electrode for the ionic liquid was also deposited onto the substrate. Polymethyl methacrylate (PMMA) resist was subsequently spun and patterned to open ‘windows’ corresponding to the MoS₂ flake, to define the region where the ionic liquid was to be in direct contact with the multilayer, that is, the region where charge accumulation occurs on application of a voltage to the gate electrode. The PMMA on top of the gate was also removed. The substrate was then mounted on a chip carrier and wire-bonded, and a small droplet of ionic liquid (DEME-TFSI, Kanto Corporation) was placed onto the device in a glove box with a controlled atmosphere (sub-ppm O₂ and H₂O concentration). The device was rapidly transferred into the variable-temperature insert (VTI) of a cryo-free Teslatron cryostat (Oxford Instruments; base temperature of 1.5 K), where it was then left in vacuum (1×10^{-6} mbar) for 1 day at room temperature to remove the oxygen and humidity present in the ionic liquid, before starting the electrical measurements.

Transport measurements. All transport measurements discussed here were performed in vacuum or a He atmosphere, inside the VTI of our Teslatron cryostat,

equipped with a 12 T superconducting magnet. To investigate superconductivity on accumulation of a high density of electrons, the device temperature was first set to 220 K, just above the freezing point of the ionic liquid, and a gate voltage was applied (typically between 2 and 5 V, depending on the device). At $T = 220$ K, possible chemical reactions between MoS₂ and the ionic liquid slow down, enabling a wider range of gate voltages to be applied without inducing device degradation. We checked that the device behaviour was reversible on repeated application of the gate voltages used in our experiments, which allowed us to rule out the occurrence of electrochemical reactions between the MoS₂ and the liquid. We also ensured that the leakage current through the ionic liquid remained negligibly small (below 1 nA) throughout the measurements, which is important because anomalous increases in leakage current are often indicative of device degradation. The reversible effect of the voltage applied to the ionic liquid gate was entirely of an electrostatic nature; intercalation in the MoS₂ can be ruled out because the molecules forming the ionic liquid are too large (nanometre size) and also because the speed with which the measured conductivity changes on the application of a gate voltage is too fast to be compatible with molecular intercalation. After having applied the gate bias, the devices were subsequently cooled down slowly to the lowest base temperature of the system. The same devices were cooled down and warmed up multiple times, changing the applied gate voltage at high temperature, without degradation. The transport characteristics were measured using a standard lock-in technique or in d.c. for I - V measurements (we used a Stanford SR830 lock-in amplifier, a Keithley 2400 source meter, and an Agilent 34401a digital multimeter, in combination with homemade low-noise voltage and current sources, as well as current/voltage amplifiers).